Available online at www.sciencedirect.com
SCIENCE DIRECT®
Journal of Sound and Vibration 273 (2004) 477–492
JOURNAL OF SOUND AND VIBRATION
www.elsevier.com/locate/jsvi

Free vibration of a rotating non-uniform beam with arbitrary pretwist, an elastically restrained root and a tip mass

Sen Yung Lee[a], Shueei Muh Lin[b,*], Ching Tien Wu[a]

[a] *Mechanical Engineering Department, National Cheng Kung University, Tainan 701, Taiwan, ROC*
[b] *Mechanical Engineering Department, Kun Shan University of Technology, Tainan 710-03, Taiwan, ROC*

Received 29 August 2002; accepted 28 April 2003

Abstract

The governing differential equations for the coupled bending–bending vibration of a rotating beam with a tip mass, arbitrary pretwist, an elastically restrained root, and rotating at a constant angular velocity, are derived by using Hamilton's principle. The frequency equation of the system is derived and expressed in terms of the transition matrix of the transformed vector characteristic governing equation. The influence of the tip mass, the rotary inertia of the tip mass, the rotating speed, the geometric parameter of the cross-section of the beam, the setting angle, and the pretwist parameters on the natural frequencies are investigated. The difference between the effects of the setting angle on the natural frequencies of pretwisted and unpretwisted beams is revealed.

1. Introduction

Rotating pretwisted beams have been used in a lot of mechanical applications such as turbine blades, helicopter rotor blades, and gear teeth. An interesting review of the subject was given by Rosen [1]. Approximation methods are very useful tools to investigate the vibrations of rotating pretwisted beams, where exact solutions are difficult to obtain even for the simplest cases. No analytical solution for the vibration of a rotating pretwisted beam had been presented.

For the non-rotating pretwisted beam, approximation methods are very useful tools to investigate the free vibrations of the pretwisted beams, where exact solutions are difficult to obtain. Dawson [2] and Dawson and Carnegie [3] used the Rayleigh–Ritz method and transformation techniques to study the effects of uniform pretwist on the frequencies of cantilever blades. Carnegie and Thomas [4] and Rao [5–7] used the Rayleigh–Ritz method and

*Corresponding author. Fax: 2734240.
E-mail address: sm.lin@msa.hinet.net (S.M. Lin).

0022-460X/03/$ - see front matter © 2003 Elsevier Ltd. All rights reserved.
doi:10.1016/S0022-460X(03)00506-6

Ritz–Galerkin method to study the effects of uniform pretwist and the taper ratio on the frequencies of cantilever blades, respectively. Gupta and Rao [8] and Abbas [9] used the finite element method to determine the natural frequencies of uniformly pretwisted tapered cantilever blading. Subrahmanyam and Rao [10] used the Reissner method to determine the natural frequencies of uniformly pretwisted tapered cantilever blading. Celep and Turhan [11] used the Galerkin method to investigate the influence of non-uniform pretwist on the natural frequencies of uniform cross-sectional cantilever or simply supported beams. Rosard and Lester [12] and Rao and Carnegie [13] used the transfer matrix method to determine the frequencies of vibration of the cantilever beam with uniform pretwist. Rosard and Lester [12] assumed that the displacements at each element are linear, Rao and Carnegie [13] used an iteration procedure to determine the displacements at each element while the initial displacements were assumed to be linear. Lin [14] used transfer matrix method to determine the natural frequencies and the associated mode shapes of any non-uniform beam with arbitrary pretwist. The exact transfer matrix was obtained.

For a rotating pretwisted beam, Subrahmanyam and Kaza [15] used the Ritz method and finite difference method to study the vibration of a cantilever tapered pretwisted beam. Sisto and Chang [16] proposed a finite element method for the vibration analysis of a rotating pretwisted beam. Hernried [17] used the finite difference method to determine the natural frequencies of a cantilever beam. Surace et al. [18] derived the approximate method based on the use of structural influence function to determine the natural frequencies of a rotating cantilever pretwisted Bernoulli–Euler beam. Young and Lin [19] used the Galerkin method to study the stability of a cantilever tapered pretwisted beam with varying speed. Lin [20] derived the frequency equation of the system which was expressed in terms of the transition matrix of the vector governing equation. Moreover, the influence of the rotary inertia and the phenomenon of divergence instability were investigated. Yoo et al. [21] used the Rayleigh–Ritz method to study the vibration of a rotating pretwisted blade with a concentrated mass. No research has been devoted to the vibration of rotating non-uniform beam with arbitrary pretwist, an elastically restrained root and tip mass.

In this paper, the governing differential equations for the coupled bending–bending–extensional vibration of a rotating non-uniform beam with a tip mass, arbitrary pretwist, an elastically restrained root, setting angle, hub radius, and rotating at a constant angular velocity, are derived by using Hamilton's principle. For an inextensional beam, without considering the Coriolis force effect, three coupled bending–bending–extensional governing differential equations are reduced to two coupled bending–bending equations and the centrifugal force is obtained. The reduced coupled governing differential equations are transformed to be a vector characteristic differential equation. The frequency equation of the system is derived and expressed in terms of the transition matrix of the vector governing equation. The efficient algorithm for determining the semi-analytical transition matrix of the system derived by Lin [20] is proposed. Finally, the influence of the tip mass, the rotating speed, the geometric parameter, the setting angle, and the pretwists on the natural frequencies are investigated.

2. Governing equations and boundary conditions

Consider the coupled bending–bending vibration of a rotating non-uniform beam with arbitrary pretwist, a tip mass and an elastically restrained root. The beam is mounted with setting

angle θ on a hub with radius R and rotates with constant angular velocity Ω, as shown in Fig. 1. The displacement fields of the beam are

$$u = u_0(x,t) - z\frac{\partial w}{\partial x} - y\frac{\partial v}{\partial x}, \quad v = v(x,t), \quad w = w(x,t), \tag{1}$$

where x, y, and z are the fixed frame co-ordinates shown in Fig. 1. t is the time variable. The velocity vector of a point (x, y, z) in the beam is given by

$$\begin{aligned}\vec{V} = &\left[\frac{\partial u}{\partial t} + \Omega\sin\theta(z+w) + \Omega\cos\theta(y+v)\right]\hat{i} \\ &+ \left[\frac{\partial v}{\partial t} - \Omega\cos\theta(x+R+u)\right]\hat{j} + \left[\frac{\partial w}{\partial t} - \Omega\sin\theta(x+R+u)\right]\hat{k}.\end{aligned} \tag{2}$$

The potential energy $\bar{U}$ and the kinetic energy $\bar{T}$ of the beam are

$$\begin{aligned}\bar{U} = &\frac{1}{2}\int_0^L \int_A \sigma_x \varepsilon_x \,\mathrm{d}A\,\mathrm{d}x + K_{z\theta}\left[\frac{\partial w(0,t)}{\partial x}\right]^2 + \tfrac{1}{2}K_{zT}w^2(0,t) \\ &+ \tfrac{1}{2}K_{y\theta}\left[\frac{\partial v(0,t)}{\partial x}\right]^2 + \tfrac{1}{2}K_{yT}v^2(0,t)\end{aligned} \tag{3}$$

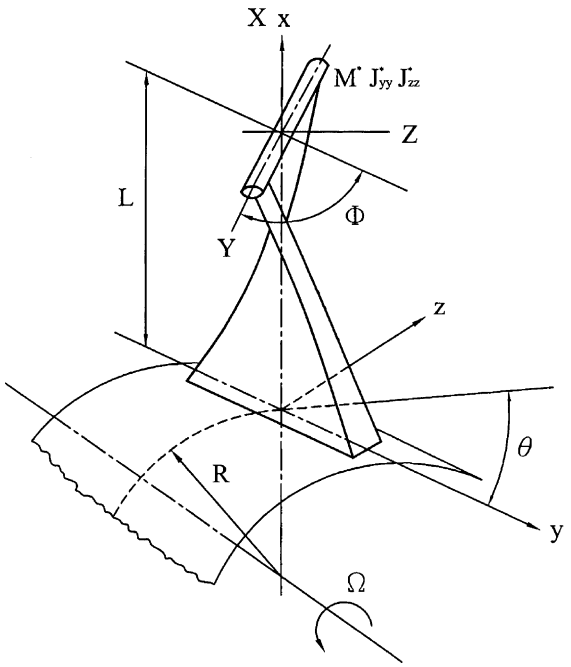

Fig. 1. Geometry and co-ordinate system of a rotating pretwisted beam.

and

$$\bar{T} = \frac{1}{2}\int_0^L \int_A \rho \vec{V}\cdot\vec{V}\,\mathrm{d}A\,\mathrm{d}x + \tfrac{1}{2}M^*[\vec{V}\cdot\vec{V}]_{x=L,\ y=0,\ z=0} + \tfrac{1}{2}J_{yy}^*\left[\Omega\sin\theta - \frac{\partial^2 w(L,t)}{\partial x\partial t}\right]^2 + \tfrac{1}{2}J_{zz}^*\left[-\Omega\cos\theta - \frac{\partial^2 v(L,t)}{\partial x\partial t}\right]^2, \tag{4}$$

where $A(x)$ is the cross-sectional area of the beam. $E(x)$ is the Young's modulus of the material. J_{yy}^* and J_{zz}^* are the rotary inertia of the tip mass about the y- and z-axis, respectively. K_{yT}, $K_{y\theta}$, K_{zT}, and $K_{z\theta}$ are the translational and rotational spring constants at the left end of the beam in the y and z directions, respectively. L is the length of the beam. M^* is the tip mass attached at the free end of the beam. $\rho(x)$ is the mass per unit volume of the beam. σ_x and ε_x are the normal stress and strain in the x direction, respectively. Application of Hamilton's principle yields the coupled governing differential equations and the elastic boundary conditions.

Consider the free bending–bending vibration of the beam without taking account of the effect of the Coriolis force and the axial neutral displacement. The dimensionless variables and parameters are defined as follows:

$$\begin{aligned}
&B_{ij}(\xi) = E(x)I_{ij}(x)/[E(0)I_{yy}(0)], && m(\xi) = \rho(x)A(x)/[\rho(0)A(0)],\\
&\bar{n}(\xi) = \alpha^2\textstyle\int_\xi^1 m(\chi)(r+\chi)\,\mathrm{d}\chi + \delta_3\alpha^2(1+r), && r = R/L,\\
&\bar{v}(\xi,\tau) = v(x,t)/L, && \bar{w}(\xi,\tau) = w(x,t)/L,\\
&\alpha^2 = \rho(0)A(0)\Omega^2L^4/[E(0)I_{yy}(0)], && \beta_1 = K_{z\theta}L/[E(0)I_{yy}(0)],\\
&\beta_2 = K_{zT}L^3/[E(0)I_{yy}(0)], && \beta_3 = K_{y\theta}L/[E(0)I_{yy}(0)],\\
&\beta_4 = K_{yT}L^3/[E(0)I_{yy}(0)], && \gamma_{i1} = \beta_i/(1+\beta_i), \quad i = 1,2,3,4,\\
&\gamma_{i2} = 1/(1+\beta_i), \quad i = 1,2,3,4, && \delta_1 = J_{yy^*}/[\rho(0)A(0)L^3],\\
&\delta_1^* = J_{YY^*}/[\rho(0)A(0)L^3], && \delta_2 = J_{zz^*}/[\rho(0)A(0)L^3],\\
&\delta_2^* = J_{ZZ^*}/[\rho(0)A(0)L^3], && \delta_3 = M^*/[\rho(0)A(0)L],\\
&\xi = x/L, && \tau = t/L^2\sqrt{E(0)I_{yy}(0)/\rho(0)A(0)},\\
&\Lambda^2 = \rho(0)A(0)\omega^2L^4/[E(0)I_{yy}(0)],
\end{aligned} \tag{5}$$

where $I_{yy}(x)$ and $I_{zz}(x)$ are the area moment of inertia of the beam section about the y- and z-axis, respectively. Consider the free vibration of the beam. The harmonic solutions can be assumed to take the form

$$\bar{w}(\xi,\tau) = W(\xi)\mathrm{e}^{\mathrm{i}\Lambda\tau}, \quad \bar{v}(\xi,\tau) = V(\xi)\mathrm{e}^{\mathrm{i}\Lambda\tau}. \tag{6}$$

The corresponding dimensionless governing differential equations of motion for harmonic vibration with circular frequency Λ can be written as

$$-\frac{\mathrm{d}^2}{\mathrm{d}\xi^2}\left(B_{yy}\frac{\mathrm{d}^2W}{\mathrm{d}\xi^2} + B_{yz}\frac{\mathrm{d}^2V}{\mathrm{d}\xi^2}\right) + \frac{\mathrm{d}}{\mathrm{d}\xi}\left(\bar{n}\frac{\mathrm{d}W}{\mathrm{d}\xi}\right) + m(\alpha^2\sin\theta + \Lambda^2)W + m\alpha^2\sin\theta\cos\theta V = 0, \tag{7}$$

$$-\frac{d^2}{d\xi^2}\left(B_{yz}\frac{d^2W}{d\xi^2}+B_{zz}\frac{d^2V}{d\xi^2}\right)+\frac{d}{d\xi}\left(\bar{n}\frac{dV}{d\xi}\right)+m(\alpha^2\cos\theta+\Lambda^2)V + m\alpha^2\sin\theta\cos\theta W=0,\quad \xi\in(0,1) \tag{8}$$

and the associated dimensionless elastic boundary conditions are as follows: At $\xi=0$,

$$\gamma_{12}\left(B_{yy}\frac{d^2W}{d\xi^2}+B_{yz}\frac{d^2V}{d\xi^2}\right)-\gamma_{11}\frac{dW}{d\xi}=0, \tag{9}$$

$$\gamma_{22}\left[\frac{d}{d\xi}\left(B_{yy}\frac{d^2W}{d\xi^2}+B_{yz}\frac{d^2V}{d\xi^2}\right)-\bar{n}\frac{dW}{d\xi}\right]+\gamma_{21}W=0, \tag{10}$$

$$\gamma_{32}\left(B_{yz}\frac{d^2W}{d\xi^2}+B_{zz}\frac{d^2V}{d\xi^2}\right)-\gamma_{31}\frac{dV}{d\xi}=0, \tag{11}$$

$$\gamma_{42}\left[\frac{d}{d\xi}\left(B_{yz}\frac{d^2W}{d\xi^2}+B_{zz}\frac{d^2V}{d\xi^2}\right)-\bar{n}\frac{dV}{d\xi}\right]+\gamma_{41}W=0. \tag{12}$$

At $\xi=1$

$$B_{yy}\frac{d^2W}{d\xi^2}+B_{yz}\frac{d^2V}{d\xi^2}-\delta_1\Lambda^2\frac{dW}{d\xi}=0, \tag{13}$$

$$\frac{d}{d\xi}\left(B_{yy}\frac{d^2W}{d\xi^2}+B_{yz}\frac{d^2V}{d\xi^2}\right)-\bar{n}\frac{dW}{d\xi} + \delta_3[(\alpha^2\sin^2\theta+\Lambda^2)W+\alpha^2\sin\theta\cos\theta V]=0, \tag{14}$$

$$B_{yz}\frac{d^2W}{d\xi^2}+B_{zz}\frac{d^2V}{d\xi^2}-\delta_2\Lambda^2\frac{dV}{d\xi}=0, \tag{15}$$

$$\frac{d}{d\xi}\left(B_{yz}\frac{d^2W}{d\xi^2}+B_{zz}\frac{d^2V}{d\xi^2}\right)-\bar{n}\frac{dV}{d\xi} + \delta_3[\alpha^2\sin\theta\cos\theta W+(\alpha^2\cos^2\theta+\Lambda^2)V]=0. \tag{16}$$

3. Solution method

Defining the state variables as

$$x_1=W,\quad x_2=\frac{dW}{d\xi},\quad x_3=\frac{d^2W}{d\xi^2},\quad x_4=\frac{d^3W}{d\xi^3},$$
$$x_5=V,\quad x_6=\frac{dV}{d\xi},\quad x_7=\frac{d^2V}{d\xi^2},\quad x_8=\frac{d^3V}{d\xi^3}. \tag{17}$$

Substituting it back to the governing characteristic differential equations (7) and (8), one obtains as follows:

$$a_1\frac{dx_4}{d\xi}+a_2\frac{dx_3}{d\xi}+a_3\frac{dx_2}{d\xi}+a_4\frac{dx_1}{d\xi^3}+a_5x_1 + a_6\frac{dx_8}{d\xi}+a_7\frac{dx_7}{d\xi}+a_8\frac{dx_6}{d\xi}+a_9\frac{dx_5}{d\xi^3}+a_{10}x_5=0, \tag{18}$$

$$a_{11}\frac{dx_4}{d\xi}+a_{12}\frac{dx_3}{d\xi}+a_{13}\frac{dx_2}{d\xi}+a_{14}\frac{dx_1}{d\xi^3}+a_{15}x_1 + a_{16}\frac{dx_8}{d\xi}+a_{17}\frac{dx_7}{d\xi}+a_{18}\frac{dx_6}{d\xi}+a_{19}\frac{dx_5}{d\xi^3}+a_{20}x_5=0, \tag{19}$$

where

$$\begin{aligned}
&a_1=B_{yy}, && a_2=2\frac{dB_{yy}}{d\xi},\\
&a_3=\frac{d^2B_{yy}}{d\xi^2}-\bar{n}, && a_4=a_{19}=-\frac{dn}{d\xi},\\
&a_5=-m(\alpha^2\sin^2\theta+\Lambda_n^2), && a_6=a_{11}=B_{yz},\\
&a_7=a_{12}=2\frac{dB_{yz}}{d\xi}, && a_8=a_{13}=\frac{d^2B_{yz}}{d\xi^2},\\
&a_9=a_{14}=0, && a_{10}=a_{15}=-m\alpha^2\sin\theta\cos\theta,\\
&a_{16}=B_{zz}, && a_{17}=2\frac{dB_{zz}}{d\xi},\\
&a_{18}=\frac{d^2B_{zz}}{d\xi^2}-\bar{n}, && a_{20}=-m(\alpha^2\cos^2\theta+\Lambda_n^2).
\end{aligned} \tag{20}$$

Multiplying Eq. (18) by a_{16} and Eq. (19) by a_6 and subtracting the latter from the former, one obtains

$$\frac{dx_4}{d\xi}=\sum_{j=1}^{8}c_jx_j, \tag{21}$$

where

$$\begin{aligned}
&c_1=-(a_5a_{16}-a_{15}a_6)/s, && c_2=-(a_4a_{16}-a_{14}a_6)/s,\\
&c_3=-(a_3a_{16}-a_{13}a_6)/s, && c_4=-(a_2a_{16}-a_{12}a_6)/s,\\
&c_5=-(a_{10}a_{16}-a_{20}a_6)/s, && c_6=-(a_9a_{16}-a_{19}a_6)/s,\\
&c_7=-(a_8a_{16}-a_{18}a_6)/s, && c_8=-(a_7a_{16}-a_{17}a_6)/s,\\
&s=a_1a_{16}-a_{11}a_6.
\end{aligned} \tag{22}$$

Similarly, multiplying Eq. (18) by a_{11} and Eq. (19) by a_1 and subtracting the latter from the former, one obtains

$$\frac{\mathrm{d}x_8}{\mathrm{d}\xi} = \sum_{j=1}^{8} \bar{c}_j x_j, \tag{23}$$

where

$$\begin{aligned}
&\bar{c}_1 = -(a_5a_{11} - a_{15}a_1)/\bar{s}, \quad \bar{c}_2 = -(a_4a_{11} - a_{14}a_1)/\bar{s},\\
&\bar{c}_3 = -(a_3a_{11} - a_{13}a_1)/\bar{s}, \quad \bar{c}_4 = -(a_2a_{11} - a_{12}a_1)/\bar{s},\\
&\bar{c}_5 = -(a_{10}a_{11} - a_{20}a_1)/\bar{s}, \quad \bar{c}_6 = -(a_9a_{11} - a_{19}a_1)/\bar{s},\\
&\bar{c}_7 = -(a_8a_{11} - a_{18}a_1)/\bar{s}, \quad \bar{c}_8 = -(a_7a_{11} - a_{17}a_1)/\bar{s},\\
&\bar{s} = a_6a_{11} - a_{16}a_1.
\end{aligned} \tag{24}$$

Based on relations (17), (21), and (23), the transformed vector characteristic governing equation can be obtained as follows:

$$\frac{\mathrm{d}\mathbf{X}(\xi)}{\mathrm{d}\xi} = \mathbf{A}(\xi)\mathbf{X}(\xi), \tag{25}$$

the state vector $\mathbf{X}(\xi)$ and system matrix $\mathbf{A}(\xi)$ are

$$\mathbf{X}(\xi) = [x_1 \quad x_2 \quad x_3 \quad x_4 \quad x_5 \quad x_6 \quad x_7 \quad x_8]^{\mathrm{T}},$$

$$\mathbf{A}(\xi) = \begin{bmatrix}
0 & 1 & 0 & 0 & 0 & 0 & 0 & 0\\
0 & 0 & 1 & 0 & 0 & 0 & 0 & 0\\
0 & 0 & 0 & 1 & 0 & 0 & 0 & 0\\
c_1 & c_2 & c_3 & c_4 & c_5 & c_6 & c_7 & c_8\\
0 & 0 & 0 & 0 & 0 & 1 & 0 & 0\\
0 & 0 & 0 & 0 & 0 & 0 & 1 & 0\\
0 & 0 & 0 & 0 & 0 & 0 & 0 & 1\\
\bar{c}_1 & \bar{c}_2 & \bar{c}_3 & \bar{c}_4 & \bar{c}_5 & \bar{c}_6 & \bar{c}_7 & \bar{c}_8
\end{bmatrix}, \tag{26}$$

the superscript T in the matrix $\mathbf{X}(\xi)$ is the transpose of a matrix.

The solution of Eq. (25) can be expressed as

$$\mathbf{X}(\xi) = \mathbf{T}(\xi, 0)\mathbf{X}(0), \tag{27}$$

where $\mathbf{T}(\xi, 0)$ is the transition matrix from 0 to ξ. After applying the composition property of the transition matrix:

$$\mathbf{T}(\xi_{i+1}, \xi_{i-1}) = \mathbf{T}(\xi_{i+1}, \xi_i)\mathbf{T}(\xi_i, \xi_{i-1}), \tag{28}$$

the transition matrix from the first subsection to the jth subsection is obtained

$$\mathbf{T}(\xi, 0) = \prod_{i=j}^{1} \mathbf{T}(\xi_i, \xi_{i-1}), \quad \xi \in (0, \xi_j). \tag{29}$$

The state variables at $\xi = 1$ can be written as

$$x_i(1) = \sum_{j=1}^{8} T_{ij}(1,0)x_j(0), \quad i = 1,2,3,\ldots,8, \tag{30}$$

where T_{ij} is the elements of the transition matrix $\mathbf{T}(\xi,0)$. The semi-analytical transition matrix derived by Lin [20] is proposed. Expressing the boundary conditions (9)–(12) in terms of the state variables $\{x_1(0), x_2(0), \ldots, x_8(0)\}$, and substituting Eq. (30) into the boundary conditions (13)–(16), the frequency equation of the system is obtained as

$$|\psi_{ij}|_{8\times 8} = 0, \quad i,j = 1,2,3,\ldots,8, \tag{31}$$

where

$$\begin{aligned}
&\psi_{11} = \psi_{14} = \psi_{15} = \psi_{16} = \psi_{18} = 0, && \psi_{12} = -\gamma_{11},\\
&\psi_{13} = \gamma_{12}B_{yy}(0), && \psi_{17} = \gamma_{12}B_{yz}(0),\\
&\psi_{21} = \gamma_{21}, && \psi_{22} = \psi_{25} = \psi_{26} = 0,\\
&\psi_{23} = \gamma_{22}B'_{yy}(0), && \psi_{24} = \gamma_{22}B_{yy}(0),\\
&\psi_{27} = \gamma_{22}B'_{yz}(0), && \psi_{28} = \gamma_{22}B_{yz}(0),\\
&\psi_{31} = \psi_{32} = \psi_{34} = \psi_{35} = \psi_{38} = 0, && \psi_{33} = \gamma_{32}B_{yz}(0),\\
&\psi_{36} = -\gamma_{31}, && \psi_{37} = \gamma_{32}B_{zz}(0),\\
&\psi_{41} = \psi_{42} = \psi_{46} = 0, && \psi_{43} = \gamma_{42}B'_{yz}(0),\\
&\psi_{44} = \gamma_{42}B_{yz}(0), && \psi_{45} = \gamma_{41},\\
&\psi_{47} = \gamma_{42}B'_{zz}(0), && \psi_{48} = \gamma_{42}B_{zz}(0),
\end{aligned}$$

$$\begin{aligned}
\psi_{5j} &= B_{yy}(1)T_{3j}(1,0) + B_{yz}(1)T_{7j}(1,0) - \Lambda_n^2\delta_1 T_{2j}(1,0), \quad j = 1,2,3,\ldots,8,\\
\psi_{6j} &= -n(1)T_{2j} + B'_{yy}(1)T_{3j}(1,0) + B_{yy}(1)T_{4j}(1,0) + B'_{yz}(1)T_{7j}(1,0)\\
&\quad + B_{yz}(1)T_{8j}(1,0) + \delta_3(\alpha^2\sin^2\theta + \Lambda_n^2)T_{1j}(1,0)\\
&\quad + \delta_3\alpha^2\sin\theta\cos\theta T_{5j}, \quad j = 1,2,3,\ldots,8,\\
\psi_{7j} &= B_{yz}(1)T_{3j}(1,0) + B_{zz}(1)T_{7j}(1,0) - \Lambda_n^2\delta_2 T_{6j}(1,0), \quad j = 1,2,3,\ldots,8,\\
\psi_{8j} &= -n(1)T_{6j} + B'_{yz}(1)T_{3j}(1,0) + B_{yz}(1)T_{4j}(1,0) + B'_{zz}(1)T_{7j}(1,0)\\
&\quad + B_{zz}(1)T_{8j}(1,0) + \delta_3\alpha^2\sin\theta\cos\theta T_{1j}(1,0)\\
&\quad + \delta_3(\alpha^2\cos^2\theta + \Lambda_n^2)T_{5j}(1,0), \quad j = 1,2,3,\ldots,8.
\end{aligned} \tag{32}$$

4. Numerical results and discussion

To illustrate the previous analysis, the performance of a rotating doubly tapered beam with arbitrary pretwist and a tip mass is studied. The corresponding parameters are

as follows:

$$B_{yy}(\xi) = \eta(1+\lambda_1\xi)^3(1+\lambda_2\xi)\sin^2\varphi + (1+\lambda_1\xi)(1+\lambda_2\xi)^3\cos^2\varphi,$$
$$B_{zz}(\xi) = \eta(1+\lambda_1\xi)^3(1+\lambda_2\xi)\cos^2\varphi + (1+\lambda_1\xi)(1+\lambda_2\xi)^3\sin^2\varphi,$$
$$B_{yz}(\xi) = 0.5[\eta(1+\lambda_1\xi)^3(1+\lambda_2\xi) - (1+\lambda_1\xi)(1+\lambda_2\xi)^3]\sin^2(2\varphi), \quad (33)$$

$$\delta_2^* = k_2\delta_3, \qquad \delta_1^* = k_1\delta_2^*,$$
$$\delta_1 = \delta_2^*\sin^2\Phi + \delta_1^*\cos^2\Phi, \quad \delta_2 = \delta_2^*\cos^2\Phi + \delta_1^*\sin^2\Phi, \quad (34)$$

where η is the square of the ratio of the width of the cross-section at the root of the beam in the y and z directions. λ_1 and λ_2 are variable rate of the width of the cross-section of the beam in the Y and Z directions, respectively. δ_1^* and δ_2^* are the dimensionless rotary inertia of the tip mass about the Y- and Z-axis, respectively.

In Table 1, the natural frequencies of rotating pretwisted beams obtained by the present method are compared with those given by Ramamurti and Kielb [22] and Yoo et al. [21] by using the Zienkiewicz's approach and the Rayleigh–Ritz method, respectively. In Table 2, the natural frequencies of unpretwisted beams obtained by the present method are compared with those given by Wright et al. [23] and Yoo et al. [21] studied the vibration of a rotating beam with a concentrated tip mass by using the Frobenius method and the Rayleigh–Ritz method, respectively. The first modes are very consistent. But the second and third modes presented are lightly smaller than those determined by the Rayleigh–Ritz method. Because the numerical result determined by the Rayleigh–Ritz method is upper bounded, the proposed method is accurate.

It should be noted that when the tip mass constant δ_3 is increased, the centrifugal force is increased. The effect of the centrifugal force is to increase the stiffness of the blade and the natural frequencies. However, the opposite effect of the tip mass constant δ_3 is to increase the total mass of the blade and to decrease the natural frequencies. The coupled effect of the tip mass and the rotational speed on the frequencies is studied here. The influence of the angular velocity α on the natural frequencies of a uniformly pretwisted cantilever beam with a concentrated tip mass is shown in Figs. 2 and 3. When tip mass constant δ_3 increases, the first and second natural frequencies decrease, and they become close as α increases. When α is smaller than a critical value,

Table 1
Comparison of the first three natural frequencies (Hz) of a rotating cantilever pretwisted beam without tip mass

	470 rpm			940 rpm		
	ω_1	ω_2	ω_3	ω_1	ω_2	ω_3
Present	18.011	90.177	261.824	24.469	97.835	271.127
[a]	19.718	91.369	263.852	28.159	100.690	272.755
[b]	19.567	90.746		28.079	100.085	

$L = 0.1524$ m, $R = 0.1016$ m, $h = 0.0254$ m, $b = 0.00127$ m, $I_{YY} = bh^3/12$, $I_{ZZ} = hb^3/12$, $E = 206.85$ GPa, $\rho = 802.73$ kg/m^3, $\theta = 0$, $\lambda_1 = 0$, $\lambda_2 = 0$, $\varphi = \xi\pi/6$.

[a] Given by Ramamurti and Kielb [22].

[b] Given by Yoo et al. [21].

Table 2
Comparison of the first three natural frequencies of a rotating unpretwisted beam with a concentrated tip mass

	$\alpha = 1$		$\alpha = 2$		$\alpha = 3$	
	Λ_1	Λ_2	Λ_1	Λ_2	Λ_1	Λ_2
Present	1.9017	16.7272	2.6696	18.0807	3.5823	20.1280
[a]	1.9017	16.7570	2.6696	18.1910	3.5823	20.3504
[b]	1.9017	16.7595	2.6696	18.1932	3.5823	20.3524

$r = 0,\ \beta_1,\ \beta_2,\ \beta_3,\ \beta_4 \to \infty,\ \delta_3 = 1,\ \eta = 1,\ \theta = 0,\ \lambda_1 = 0,\ \lambda_2 = 0,\ \varphi = 0,\ k_1 = 0,\ k_2 = 0.$
[a] Given by Wright et al. [23].
[b] Given by Yoo et al. [21].

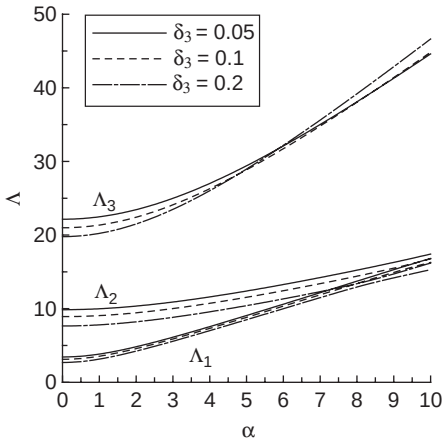

Fig. 2. The influence of the angular velocity α on the natural frequencies with various tip mass δ_3 ($r = 1$; $\beta_1,\ \beta_2,\ \beta_3,\ \beta_4 \to \infty$; $\eta = 10$; $\theta = 0$; $\lambda_1 = -0.1,\ \lambda_2 = -0.1$; $\varphi = \xi\pi/4$; $k_1 = 0,\ k_2 = 0$).

the third natural frequency decreases as δ_3 increases. However, when α is larger than the critical value, the third natural frequency increases as δ_3 is increased. The reason is that for a small rotational speed the influence of the inertia on the frequencies is greater than that of the centrifugal force. However, the centrifugal force includes the term of the product of the rotating speed and the tip mass constant. For a large rotational speed the centrifugal force is increased greatly and the natural frequencies will be increased. Figs. 3 shows that for a small rotating speed when δ_3 is increased, the first three natural frequencies are decreased. But for a large rotating speed if δ_3 exceeds a critical value, the influence of centrifugal force on the third natural frequency is greater than that of the inertia of tip mass δ_3. In other words, when δ_3 is increased over the critical value, the third frequency is increased.

In Figs. 4a and b, the influence of the angular velocity α on the natural frequencies of a cantilever beam pretwisted uniformly and non-uniformly are shown, respectively. It can be observed in Fig. 4a that for a uniformly pretwisted beam the influence of Φ on the third natural frequency is greater than on the first and second ones. The influence on the second and third

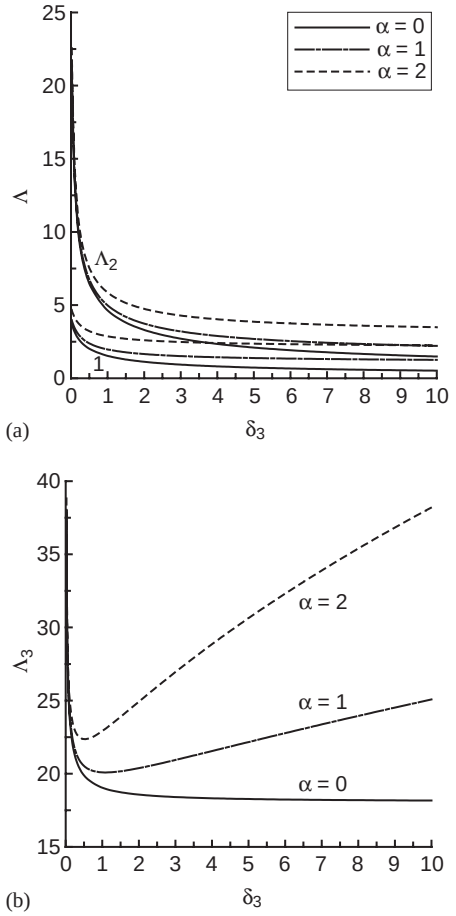

Fig. 3. (a) The influence of the tip mass δ_3 on the first and second natural frequencies with various angular velocity α ($r = 1$; β_1, β_2, β_3, $\beta_4 \to \infty$; $\eta = 10$; $\theta = \pi/2$; $\lambda_1 = -0.1$, $\lambda_2 = -0.1$; $\varphi = \xi\pi/4$; $k_1 = 0$, $k_2 = 0$). (b) The influence of the tip mass δ_3 on the third natural frequency with various angular velocity α ($r = 1$; β_1, β_2, β_3, $\beta_4 \to \infty$; $\eta = 10$; $\theta = \pi/2$; $\lambda_1 = -0.1$, $\lambda_2 = -0.1$; $\varphi = \xi\pi/4$; $k_1 = 0$, $k_2 = 0$).

natural frequencies will decrease as α is increased. It can be observed in Fig. 4b that for non-uniform pretwist when α is increased, the influence of Φ on the first natural frequency increases, but the influence on the third natural frequency decreases. Moreover, the veering phenomenon of second natural frequency is observed: when α is less than 5, the influence of Φ on the second natural frequency decreases, but the influence increases if α is greater than 5.

In Table 3, the influence of the setting angle θ and the total pretwist angle Φ on the first two natural frequencies of a cantilever beam is shown. When the setting angle is increased, the frequencies of the unpretwisted beam, i.e., $\Phi = 0^0$, are decreased. The phenomenon is the same as that studied by Lee and Lin [24]. However, when the setting angle is increased, the first frequencies of the pretwisted beams are initially increased and then decreased. Meanwhile, the second frequencies are increased. The reason is given as following:

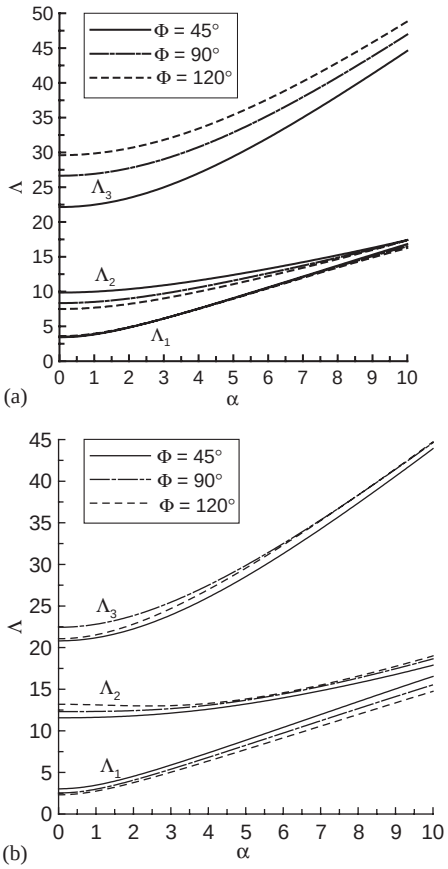

Fig. 4. (a) The influence of the angular velocity α on the natural frequencies with various tip pretwist angle Φ of uniform pretwist ($r = 1$; β_1, β_2, $\beta_3, \beta_4 \to \infty$; $\delta_3 = 0.05$; $\eta = 10$; $\theta = 0$; $\lambda_1 = -0.1$, $\lambda_2 = -0.1$; $\varphi = \Phi\xi$; $k_1 = 0$, $k_2 = 0$). (b) The influence of the angular velocity α on the natural frequencies with various tip pretwist angle Φ of non-uniform pretwist ($r = 1$; β_1, β_2, β_3, $\beta_4 \to \infty$; $\delta_3 = 0.05$; $\eta = 10$; $\theta = 0$; $\lambda_1 = -0.1$, $\lambda_2 = -0.1$; $\varphi = \Phi \sin(\pi\xi/2)$; $k_1 = 0$, $k_2 = 0$).

Without the account of pretwist, Eq. (7) becomes the governing equation of an unpretwisted beam given by Lee and Lin [24]

$$\frac{\mathrm{d}^2}{\mathrm{d}\xi^2}\left(B_{yy}\frac{\mathrm{d}^2 W}{\mathrm{d}\xi^2}\right) - \frac{\mathrm{d}}{\mathrm{d}\xi}\left(\bar{n}\frac{\mathrm{d}W}{\mathrm{d}\xi}\right) - m(\alpha^2 \sin^2\theta + \Lambda^2)W = 0. \tag{35}$$

The last term of Eq. (35) is an inertial one. When the setting angle is increased, the coupling inertia effect of the mass and the setting angle is increased and the natural frequencies are decreased [24]. For a rotating pretwisted beam the last second term of Eq. (7) $m\alpha^2 \sin^2\theta$ are two coupling inertia of the mass and the setting angle. When the setting angle θ increases, the coupling inertia effect increases. However, when the setting angle θ increases, the coupling inertia term of Eq. (8) $m\alpha^2 \cos^2\theta$ decreases. Moreover, when the setting angle θ increases from zero to $\pi/4$, the last inertia terms of Eqs. (7) and (8) $m\alpha^2 \sin\theta\cos\theta$ increases. When the setting angle θ increases from $\pi/4$ to $\pi/2$, the inertia terms decreases. The difference between the coupling inertia term of a

Table 3
Effect of the setting angle θ on the dimensionless frequencies of a rotating pretwisted cantilever beam

θ	Λ_1 (deg)			Λ_2 (deg)		
	$\Phi = 0$	$\Phi = 45$	$\Phi = 60$	$\Phi = 0$	$\Phi = 45$	$\Phi = 60$
0	4.210	4.285	4.420	22.575	18.146	16.092
10	4.206	4.289	4.426	22.574	18.272	16.239
20	4.196	4.289	4.430	22.572	18.645	16.685
30	4.180	4.284	4.431	22.569	19.260	17.450
40	4.160	4.275	4.429	22.566	20.099	18.555
50	4.139	4.264	4.423	22.562	21.108	19.998
60	4.120	4.250	4.415	22.558	22.186	21.701
70	4.103	4.237	4.406	22.555	23.169	23.434
80	4.093	4.226	4.396	22.553	23.866	24.784
90	4.089	4.218	4.388	22.553	24.118	25.299

$B_{yy} = (1 - 0.1\xi)^4 \cos^2 \xi\Phi + 200(1 - 0.1\xi)^4 \sin^2 \xi\Phi$, $B_{zz} = 200(1 - 0.1\xi)^4 \cos^2 \xi\Phi + (1 - 0.1\xi)^4 \sin^2 \xi\Phi$,
$B_{yz} = 49.5(1 - 0.1\xi)^4 \sin 2\xi\Phi$, $r = 1$, $\alpha = 1$.

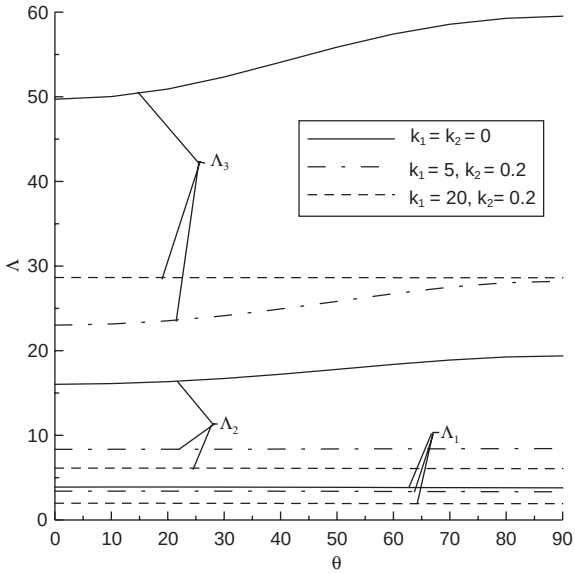

Fig. 5. The influence of the setting angle θ on the first three frequencies with various parameters of rotary inertias of tip mass k_1, k_2 ($r = 1$; $\alpha = 1$; β_1, β_2, β_3, $\beta_4 \to \infty$; $\eta = 200$; $\lambda_1 = -0.1$, $\lambda_2 = -0.1$; $\varphi = \xi\pi/4$, $\delta_3 = 0.05$).

unpretwisted beam and those of a pretwisted beam is revealed. Further, it is found that when the setting angle is increased, the natural frequencies of a unpretwisted beam must be decreased, but those of a pretwisted beam may be increased.

Fig. 5 shows the influence of the setting angle θ on the natural frequencies of a cantilever beam pretwisted uniformly, with various parameters of the rotary inertia of the tip mass, k_1 and k_2. It can be observed that there is almost no effect of the setting angle on the first natural frequency. When the setting angle is increased, the second and third frequencies are increased. When the

rotary inertia constants k_1 and k_2 are increased, the natural frequencies are decreased. Moreover, the rotary inertia about the Y-axis will greatly decrease the effect of the setting angle on the frequencies.

Fig. 6 shows the influence of the root spring constants β_i on the first three natural frequencies of a pretwisted beam with the parameters $\{r = 1, \delta_3 = 0.05, \eta = 10, \theta = 0, \lambda_1 = -0.1, \lambda_2 = -0.1, \varphi = \xi\pi/4, k_1 = 0, k_2 = 0\}$. Figs. 6a and b show that the influence of the rotational root spring constants on the natural frequencies is very small. However, Figs. 6c and d show that the influence of the translational root spring constants on especially the fundamental frequency is large. It is well known [22] that if the fundamental frequency is decreased to zero, the divergence instability will happen. Lin [22] revealed that the divergence instability will not happen to a pretwisted Bernoulli–Euler beam with $r > 0$, $\theta < \pi/4$, β_2, $\beta_4 \to \infty$, $\beta_1 > 0$, and $\beta_3 > 0$ and a unpretwisted Bernoulli–Euler beam with β_2, $\beta_4 \to \infty$ and $r > 0$. However, the divergence instability will happen to both pretwisted and unpretwisted beams with infinite rotational root spring constants β_1, β_3 when the translational root spring constants β_2 and β_4 are smaller than some critical values. Fig. 6 verifies the facts that the effects of the translational root spring constants on the frequencies are greatly larger than those of the rotational root spring constants.

5. Conclusion

In this paper, a solution procedure for the bending–bending vibration of a rotating non-uniform beam with arbitrary pretwist and an elastically restrained root is derived. A simple and efficient algorithm for deriving the semi-analytical transition matrix of the general system with non-uniform pretwist is proposed. The accurate natural frequencies and mode shapes of the beam with elastic root can be obtained. Based on the facts, one can derives the analytical solution for the forced vibration of the system by using the method of mode superposition. However, it is difficult to determine the frequencies and the mode shapes of a beam with elastic root by using the approximate methods such as Ritz method and FEM. The influence of the tip mass, the rotary inertia of the tip mass, the rotating speed, the geometric parameter, the setting angle, and the pretwist angle on the natural frequencies are investigated. It is shown that

1. For a small rotating speed when the tip mass parameter δ_3 is increased, the first three natural frequencies are decreased. But for a large rotating speed when δ_3 exceeds a critical value, the influence of centrifugal force on the third natural frequency is greater than that of the inertia of tip mass δ_3. In other words, when δ_3 is increased over the critical value, the third frequency is increased.
2. The effects of the pretwist angle on the natural frequencies of lower modes of the beam with uniform pretwist and on those of the beam with non-uniform pretwist are almost same. But the effects of the pretwist angle on the natural frequencies of higher modes of the beam with uniform pretwist and on those of the beam with non-uniform pretwist are different greatly.
3. Lee and Lin [24] found that the natural frequencies of a rotating unpretwisted beam would decrease as the setting angle is increased. However, the natural frequencies of a rotating pretwisted beam may be increased or decreased as the setting angle is increased. Moreover, the rotary inertias of the tip mass will decrease the influence of the setting angle on the natural frequencies.

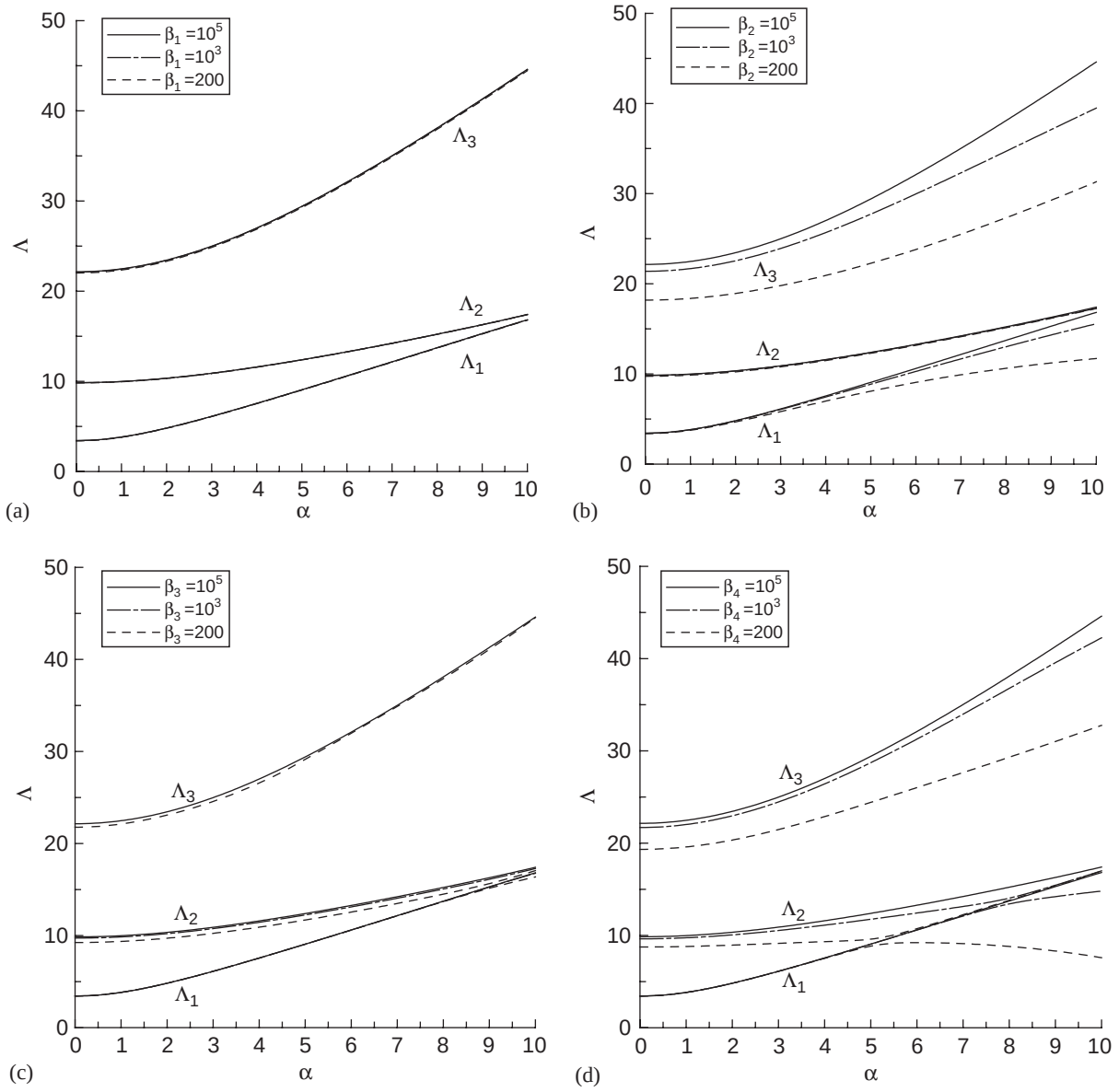

Fig. 6. (a) The influence of the angular velocity α and the rotational root spring constant β_1 on the natural frequencies ($r = 1;\ \beta_2,\ \beta_3,\ \beta_4 \to \infty;\ \delta_3 = 0.05;\ \eta = 10;\ \theta = 0;\ \lambda_1 = -0.1,\ \lambda_2 = -0.1;\ \varphi = \xi\pi/4;\ k_1 = 0,\ k_2 = 0$). (b) The influence of the angular velocity α and the translational root spring constant β_2 on the natural frequencies ($r = 1;\ \beta_1,\ \beta_3,\ \beta_4 \to \infty;\ \delta_3 = 0.05;\ \eta = 10;\ \theta = 0;\ \lambda_1 = -0.1,\ \lambda_2 = -0.1;\ \varphi = \xi\pi/4;\ k_1 = 0,\ k_2 = 0$). (c) The influence of the angular velocity α and the rotational root spring constant β_3 on the natural frequencies ($r = 1;\ \beta_1,\ \beta_2,\ \beta_4 \to \infty;\ \delta_3 = 0.05;\ \eta = 10;\ \theta = 0;\ \lambda_1 = -0.1,\ \lambda_2 = -0.1;\ \varphi = \xi\pi/4;\ k_1 = 0,\ k_2 = 0$). (d) The influence of the angular velocity α and the translational root spring constant β_4 on the natural frequencies ($r = 1;\ \beta_1,\ \beta_2,\ \beta_3 \to \infty;\ \delta_3 = 0.05;\ \eta = 10;\ \theta = 0;\ \lambda_1 = -0.1,\ \lambda_2 = -0.1;\ \varphi = \xi\pi/4;\ k_1 = 0,\ k_2 = 0$).

References

[1] A. Rosen, Structural and dynamic behavior of pretwisted rods and beams, *Applied Mechanics Review* 44 (12) (1991) 483–515.
[2] B. Dawson, Coupled bending vibrations of pretwisted cantilever blading treated by Rayleigh–Ritz method, *Journal of Mechanical Engineering Science* 10 (5) (1968) 381–386.
[3] B. Dawson, W. Carnegie, Modal curves of pre-twisted beams of rectangular cross-section, *Journal of Mechanical Engineering Science* 11 (1) (1969) 1–13.
[4] W. Carnegie, J. Thomas, The coupled bending–bending vibration of pre-twisted tapered blading, *Journal of Engineering Industry* 94 (1) (1972) 255–266.
[5] J.S. Rao, Flexural vibration of pretwisted tapered cantilever blades, *Journal of Engineering Industry* 94 (1) (1972) 343–346.
[6] J.S. Rao, Coupled vibrations of turbomachine blading, *Shock and Vibration Bulletin* 47 (1977) 107–125.
[7] J.S. Rao, *Advanced Theory of Vibration*, Wiley, New York, 1992, pp. 330–338.
[8] R.S. Gupta, J.S. Rao, Finite element eigenvalue analysis of tapered and twisted Timoshenko beams, *Journal of Sound and Vibration* 56 (2) (1978) 187–200.
[9] B. Abbas, Simple finite elements for dynamic analysis of thick pre-twisted blades, *Aeronautical Journal* 83 (1979) 450–453.
[10] K.B. Subrahmanyam, J.S. Rao, Coupled bending–bending cantilever beams treated by the Reissner method, *Journal of Sound and Vibration* 82 (4) (1982) 577–592.
[11] Z. Celep, D. Turhan, On the influence of pretwisting on the vibration of beams including the shear and rotary inertia effects, *Journal of Sound and Vibration* 110 (3) (1986) 523–528.
[12] D.D. Rosard, P.A. Lester, Natural frequencies of twisted cantilever beams, *American Socitey of Mechanical Engineers, Journal of Applied Mechanics* 20 (1953) 241–244.
[13] J.S. Rao, W. Carnegie, A numerical procedure for the determination of the frequencies and mode shapes of lateral vibration of blades allowing for the effect of pre-twist and rotation, *International Journal of Mechanical Engineering Education* 1 (1) (1973) 37–47.
[14] S.M. Lin, Vibrations of elastically restrained nonuniform beams with arbitrary pretwist, *American Institute of Aeronautics and Astronautics Journal* 35 (11) (1997) 1681–1687.
[15] K.B. Subrahmanyam, K.R.V. Kaza, Vibration and buckling of rotating, pretwisted, preconed beams including coriolis effects, *American Socitey of Mechanical Engineers, Journal of Vibration, Acoustics, Stress, and Reliability in Design* 108 (2) (1986) 140–149.
[16] F. Sisto, A.T. Chang, Finite element for vibration analysis of twisted blades based on beam theory, *American Institute of Aeronautics and Astronautics Journal* 22 (11) (1984) 1646–1651.
[17] A.G. Hernried, Forced vibration response of a twisted non-uniform rotating blade, *Computers and Structures* 41 (2) (1991) 207–212.
[18] G. Surace, V. Anghel, C. Mares, Coupled bending–bending–torsion vibration analysis of rotating pretwisted blades: an integral formulation and numerical examples, *Journal of Sound and Vibration* 206 (4) (1997) 473–486.
[19] T.H. Young, T.M. Lin, Stability of rotating pretwisted, tapered beams with randomly varying speeds, *American Society of Mechanical Engineers, Journal of Vibration and Acoustics* 120 (3) (1998) 784–790.
[20] S.M. Lin, The instability and vibration of rotating beams with arbitrary pretwist and an elastically restrained root, *American Society of Mechanical Engineers, Journal of Applied Mechanics* 68 (2001) 844–853.
[21] H.H. Yoo, J.Y. Kwak, J. Chung, Vibration analysis of rotating pre-twisted blades with a concentrated mass, *Journal of Sound and Vibration* 240 (5) (2001) 891–908.
[22] V. Ramamurti, R. Kielb, Natural frequencies of twisted rotating plates, *Journal of Sound and Vibration* 97 (3) (1984) 429–449.
[23] A.D. Wright, C.E. Smith, R.W. Thresher, J.L.C. Wang, Vibration modes of centrifugally stiffened beams, *American Society of Mechanical Engineers, Journal of Applied Mechanics* 49 (1982) 197–202.
[24] S.Y. Lee, S.M. Lin, Bending vibrations of rotating nonuniform Timoshenko beams with an elastically restrained root, *American Society of Mechanical Engineers, Journal of Applied Mechanics* 61 (1994) 949–955.